Synthesis of biodiesel from *Jatropha curcas* L. seed oil using artificial zeolites loaded with CH₃COOK as a heterogeneous catalyst

Wei Xue[1], You-Chun Zhou[1], Bao-An Song[1], Xia Shi[1], Jun Wang[1], Shi-Tao Yin[1], De-Yu Hu[1], Lin-Hong Jin[1], Song Yang[1,*]

[1]Key Laboratory of Green Pesticide and Bioengineering, Ministry of Education of China, Center for Research and Development of Fine Chemicals, Guizhou University, Guiyang 550025, P. R. China; To whom correspondence should be addressed: Tel.: +86-851-362-0521, Fax: +86-851-362-2211.
Email: *jhzx.msm@gmail.com, *yangsdqj@gmail.com

ABSTRACT

An environmentally benign process was developed for the transesterification of *Jatropha curcas* L. seed oil with methanol using artificial zeolites loaded with potassium acetate as a heterogeneous catalyst. After calcination for 5 h at 823 K, the catalyst loaded with 47 wt.% CH₃COOK exhibited the highest efficiency and best catalytic activity. The easily prepared catalysts were characterized by means of X-ray diffraction and IR spectroscopy, as well as Hammett indicator titration. The results revealed a strong dependence of catalytic activity on basicity. The optimum reaction conditions for transesterification of J. curcas oil were also investigated. The methyl ester content in the biodiesel product exceeded 91% after 4h reaction at reflux temperature in the presence of 2% solid catalyst and no water washing process is needed during workup.

Keywords: Biodiesel; Heterogeneous Catalyst; Artificial Zeolites; *Jatropha Curcas* L. seed Oil

1. INTRODUCTION

Biodiesel is a biodegradable and non-toxic renewable alternative to diesel fuel that is composed of mono-alkyl esters of long-chain fatty acids derived from vegetable oils or animal fats. Biodiesel is increasing in importance because of its benign impact on the environment. [1,2] Biodiesel is produced mainly through the transesterification of vegetable oils using short-chain alcohols, typically methanol or ethanol [3], because these are cheap and readily available from syngas, in which methanol is usually preferred. [4,5] Transesterification of vegetable oils with methanol, also called methanolysis, is typically carried out in the presence of homogeneous base or acid catalysts. Homogeneous base catalysts, including potassium hydroxide, sodium hydroxide and potassium and sodium alkoxides, such as NaOCH₃ [1], have higher catalytic activity than acid catalysts. Furthermore, since acid catalysts are more corrosive than base catalysts, base catalysis is usually preferred in commercial processes. [6] In the conventional homogeneous reaction, removal of the base after reaction is a major problem, since aqueous quenching results in the formation of stable emulsions and saponification, making the separation of methyl esters difficult and producing waste water. [7] However, the use of solid base catalysts can not only overcome those disadvantages, but also confer some advantages, such as the elimination of a quenching step (and associated contaminated water waste) during the work-up process and the scope to operate in continuous mode. [8,9] Therefore, environmentally friendly heterogeneous catalysts are promising for biodiesel production because of environmental constraints and potential simplification of existing processes.

Recently, heterogeneous catalysts used to catalyze the transesterification of vegetable oils to prepare fatty acid methyl esters (FAME) have attracted considerable attention. Wilson *et al.* [5] prepared a series of Li-promoted CaO catalysts with Li loading in the range 0.26−4.0 wt.% to catalyze the transesterification of glyceryl tributyrate and methanol. They found that the optimum loading correlated with the formation of an electron-deficient surface Li⁺ species and associated-OH species at defect sites on the support. Lee *et al.* [10] reported a process for the production of biodiesel from vegetable oils using an Na/NaOH/γ-Al₂O₃ heterogeneous catalyst. Under optimized reaction conditions, this Na/NaOH/γ-Al₂O₃ heterogeneous base catalyst showed almost the same activity as a conventional homogeneous NaOH catalyst. However, the base catalyst had to be

prepared in special apparatus equipped with a nitrogen flow line and cold circulating water flow. These disadvantages restrict potential industrial applications. Xie *et al*. [11] developed a type of Al_2O_3-loaded KNO_3 solid base catalyst for the transesterification of soybean oil. The catalytic activity was ascribed to the presence of K_2O and K-O-Al groups derived from KNO_3 or other potassium compounds during high-temperature calcination.

Zeolites have attracted much attention in the preparation of solid base catalysts. [12,13,14,15] The basicity and catalytic activity of these zeolites can be modulated through ion exchange of alkali and the occlusion of alkali metal oxides in zeolite cages by decomposition. However, the preparation procedures for these modified zeolites have some disadvantages. For ion-exchanged zeolites, the exchanged samples need to be washed with distilled, deionized water to remove excess alkali remaining in the ETS-10 zeolite cages. [13] Furthermore, the treatment process requires a long time and produces much waste water.

In the present study, a modified artificial zeolite for catalysis of the transesterification of *Jatropha curcas* L. seed oil was developed using a simple preparation process. This catalyst preparation technique has many advantages: (1) compared with ETS-10 and NaX zeolites, artificial zeolites are cheaper; (2) artificial zeolites are used directly as a support without any pretreatment; and (3) after impregnation with potassium acetate, artificial zeolite samples were dried and then simply calcined in a muffle furnace. Unlike NaX occluded catalysts, [13,14] artificial zeolite-supported potassium acetate was thermally decomposed in an uncontrolled manner and the catalyst sample was prepared easily. To the best of our knowledge, this is the first time that a catalyst of artificial zeolites loaded with CH_3COOK has been adopted for biodiesel production from *J. curcas* oil, a plant belonging to the Euphorbiaceae family with seed oil that is non-edible and a good material for industrial biodiesel production. [16] After calcination for 5 h at 823 K, the artificial zeolite catalyst loaded with 47 wt.% CH_3COOK exhibited the highest basicity and the best catalytic activity for the reaction. The catalytic activity was evaluated in terms of the methyl ester content of the product after transesterification of *J. curcas* oil. The optimum reaction conditions were determined using an orthogonal experimental method.

2. EXPERIMENTAL

2.1. Catalyst Preparation

Artificial zeolites ($Na_2O \cdot Al_2O_3 \cdot xSiO_2 \cdot yH_2O$) were obtained from Shanghai Qingxi Chemical Science and Technology Ltd. (Shanghai, China). CH_3COOK/artificial zeolite supported catalysts were prepared by impregnating artificial zeolites with an aqueous solution of potas-

sium acetate. Samples with various CH_3COOK loadings were impregnated for 12 h to ensure that the CH_3COOK diffused and dispersed thoroughly over the surface and through the pores of the artificial zeolites. The samples were then dried overnight at 383 K and calcined (typically at 823 K) in air for 5 h to yield readily usable catalysts. In experiments, catalyst samples with loading amounts of 9,23,33,41,44,47 and 50 wt.% (relative to the total mass of the catalyst before calcination) were designated as 9%, 23%, 33%, 41%, 44%, 47% and 50% CH_3COOK/artificial zeolites, respectively. [11]

2.2. Catalyst Characterization

The basic strength (H_) of the solid base was assessed using Hammett indicators. [17,18,19] In our experiments, the following Hammett indicators were used: bromthymol blue (H_=7.2), phenolphthalein (H_=9.8), 2, 4-dinitroa-niline (H_=15.0), and nitroaniline (H_=18.4). Approximately 50 mg of the catalyst sample was shaken with 10 mL of anhydrous ethanolic solution of Hammett indicator and left to equilibrate for 2 h. [20] Then the color change of the solution was observed. When the solution exhibits a color change, this indicates that the basic strength of the catalyst is stronger than the indicator used. However, when the solution produces no color change, the basic strength of the catalyst is weaker than that of the indicator used. The basicity of the catalysts was determined by titration with a Hammett indicator and a 0.02 mol/L anhydrous ethanolic solution of benzene carboxylic acid. [6] It should be noted that Hammett indicator titration can only give qualitative information about the basic properties of catalysts.

X-Ray diffraction (XRD) patterns of the samples were recorded on a Rigaku D/MAX-2200 powder X-ray diffractometer with Cu K_α (λ=0.154nm) radiation using an acceleration voltage of 40 kV and a current of 30mA, over a 2θ range of 0-65° with a step size of 0.04° at a scanning speed of 3°/min. The data were processed using DiffracPlus software. The phases were identified using the Power Diffraction File (PDF) database (JCPDS, International Center for Diffraction Data).

IR spectra of the samples were measured using the KBr pellet technique. Spectra were recorded on a Shimadzu IR-Prestige-21 spectrometer with resolution of 4 cm^{-1} over the range 400-4000cm^{-1}.

2.3. Transesterification Reaction

Jatropha curcas oil was prepared by squeezing seeds of J. curcas from Luodian county, Guizhou Province, southwest China. The crude oil obtained was then further purified by filtering out solid impurities and refined to reduce the water content. According to gas chromatography (GC) analysis, the fatty acids of *J. curcas* oil consisted of: palmitic acid (12.47%), palmitoleic acid (2.10%), stearic acid (6.42%), oleic acid (32.04%), and

linoleic acid (42.47%). The acid value of the oil was approximately 2.63mg KOH/g, and an average molecular weight of 880g/mol was calculated from the saponification value (Sv=194mg KOH/g).

A 250-mL three-necked glass flask equipped with a water-cooled condenser, thermometer and magnetic stirrer was charged with 110.0g (125mmol, calculated from the average molecular weight) of *J. curcas* oil, different volumes of methanol and various amounts of catalyst. The mixture was vigorously stirred and refluxed for the required reaction time. After completion of methanolysis, the mixture was filtered and excess methanol was recovered by rotary evaporation. The liquid phase was transferred into a separatory funnel and allowed to settle; the upper layer, the biodiesel product, was analyzed by GC.

2.4. Analysis Methods

The external standard method was adopted for GC product analysis. An Agilent 6890GC instrument equipped with a flame ionization detector was used. The chromatographic conditions were as follows: column, HP-Innowax (30m× 0.32mm, 0.25μm); inlet temperature, 523K; detector temperature, 523K; split ratio, 20:1; oven temperature program, 463K for 3min, ramp at 15K/min to 513K, hold for 8min; injection volume, 1μL; carrier gas, N_2 at 1.0mL/min; air flow, 450mL/min; H_2 flow, 40mL/min.

3. RESULTS AND DISCUSSION

3.1. Basic Strength of the Catalyst

Table 1 shows the basic strength of the parent artificial zeolite (entry 1) and various CH_3COOK/artificial zeolite catalysts calcined at different temperatures. The basic

strength of catalyst samples with CH_3COOK loading of ＜33wt.% and calcined at 823 K are in the range 7.2<H_ ＜9.8 (entries 2−4). The basic strength increased to 15.0＜ H_＜18.4 when the CH_3COOK loading exceeded 33 wt.% (entries 5−＜9). This indicates that there are at least two types of active base sites in the supported catalysts.

For loading of <33wt.%, the amount of CH_3COOK is not enough to cover all of the support surface and incorporation of potassium ions into the vacancies of the support is mainly through strong salt-support or oxide-support interaction. [20] New active base species emerge when CH_3COOK loading exceeds 33wt.%, indicating that $(CH_3COOK)_n$ -support interaction plays an important role in this process. However, the basic strength of 47 wt.% CH_3COOK/artificial zeolite calcined at a temperature less than 623 K showed no increase compared with the artificial zeolite (entries 1, 10, 11). This is likely because CH_3COOK loaded onto the artificial zeolite is not decomposed at temperature less than 623 K. The catalysts calcined between 623 and 973 K exhibit similar basic strength (entries 12-15). According to the definition of Tanabe, [21] these catalyst samples, with base strength in the range 15.0＜H_＜18.4, can be regarded as strong bases.

3.2. Basicity of the Catalyst

Table 2 summarizes the basicity of a series of CH_3COOK/artificial zeolite catalysts calcined at different temperatures, as determined using Hammett indicators. As shown in **Table 2**, the basicity of catalysts calcined at 823 K first increases and then decreases with the increasing CH_3COOK loading (entries 2−8), with 47 wt.% CH_3COOK/artificial zeolite exhibiting the highest

Table 1. Basic strength of various CH_3COOK/artificial zeolite catalysts calcined at different temperatures.

Entry	Samples	Calcination temperature (K)	Basic strength (H_)
1	Artificial zeolite	−	7.2<H_＜9.8
2	Artificial zeolite	823	7.2<H_＜9.8
3	9%CH_3COOK/artificial zeolite	823	7.2<H_＜9.8
4	23%CH_3COOK/artificial zeolite	823	7.2<H_＜9.8
5	33%CH_3COOK/artificial zeolite	823	15.0<H_＜18.4
6	41%CH_3COOK/artificial zeolite	823	15.0<H_＜18.4
7	44%CH_3COOK/artificial zeolite	823	15.0<H_＜18.4
8	47%CH_3COOK/artificial zeolite	823	15.0<H_＜18.4
9	50%CH_3COOK/artificial zeolite	823	15.0<H_＜18.4
10	47%CH_3COOK/artificial zeolite	−	7.2<H_＜9.8
11	47%CH_3COOK/artificial zeolite	523	7.2<H_＜9.8
12	47%CH_3COOK/artificial zeolite	623	15.0<H_＜18.4
13	47%CH_3COOK/artificial zeolite	723	15.0<H_＜18.4
14	47%CH_3COOK/artificial zeolite	923	15.0<H_＜18.4
15	47%CH_3COOK/artificial zeolite	973	15.0<H_＜18.4

Table 2. Basicity of various CH_3COOK/artificial zeolite catalysts calcined at different temperatures.

Entry	Samples	Calcination temperature (K)	Basicity (mmol KOH/g)
1	Artificial zeolite	–	0
2	Artificial zeolite	873	0
3	9%CH_3COOK/artificial zeolite	823	0.0246
4	23%CH_3COOK/artificial zeolite	823	0.1393
5	33%CH_3COOK/artificial zeolite	823	0.3122
6	41%CH_3COOK/artificial zeolite	823	0.3527
7	47%CH_3COOK/artificial zeolite	823	0.4058
8	50%CH_3COOK/artificial zeolite	823	0.3786
9	47%CH_3COOK/artificial zeolite	–	0.2079
10	47%CH_3COOK/artificial zeolite	523	0.2540
11	47%CH_3COOK/artificial zeolite	623	0.2832
12	47%CH_3COOK/artificial zeolite	723	0.3689
13	47%CH_3COOK/artificial zeolite	923	0.2956
14	47%CH_3COOK/artificial zeolite	973	0.1654

basicity (0.4058 mmol KOH/g; entry 7). This is similar to the findings of Xie *et al*. [11] The calcination temperature also affects catalyst basicity. It is evident from **Table 2** that catalysts calcined at 823K had the highest basicity (entries 7, 9−14). It was noted that 47% CH_3COOK/artificial zeolite without calcination had higher basicity than 23% CH_3COOK/artificial zeolite calcined at 823 K (0.2079 vs. 0.1393 mmol KOH/g, entries 9 and 4).

3.2 Basicity of the Catalyst

Table 2 summarizes the basicity of a series of CH_3COOK/artificial zeolite catalysts calcined at different temperatures, as determined using Hammett indicators. As shown in **Table 2**, the basicity of catalysts calcined at 823 K first increases and then decreases with the increasing CH_3COOK loading (entries 2−8), with 47 wt.% CH_3COOK/artificial zeolite exhibiting the highest basicity (0.4058 mmol KOH/g; entry 7). This is similar to the findings of Xie *et al*. [11] The calcination temperature also affects catalyst basicity. It is evident from **Table 2** that catalysts calcined at 823 K had the highest basicity (entries 7, 9−14). It was noted that 47% CH_3COOK/artificial zeolite without calcination had higher basicity than 23% CH_3COOK/artificial zeolite calcined at 823 K (0.2079 vs. 0.1393 mmol KOH/g, entries 9 and 4).

3.3. Lnfluence of Catalyst Preparation Conditions

3.3.1. Lnfluence of CH_3COOK Loading
The catalytic activity of the catalysts was evaluated by comparing the FAME content of the transesterification products. The effect of CH_3COOK loading on the cata-

lytic activity is shown **Fig. 1**. As the CH_3COOK loading increases from 9% to 47%, the methyl ester content increases. The highest methyl ester content (91.58%) was obtained for 47 wt.% CH_3COOK loading. However, the FAME content decreased slightly for a further increase in CH_3COOK loading, which may be due to partial covering of basic sites by K_2O species from the excess CH_3COOK on the surface of the composite. It is important to point out that the conversion decreased significantly when potassium salt loading exceeded the critical limit for the transesterification of soybean. [11]

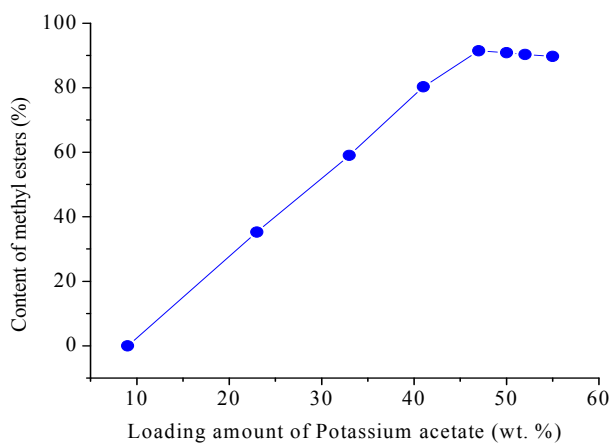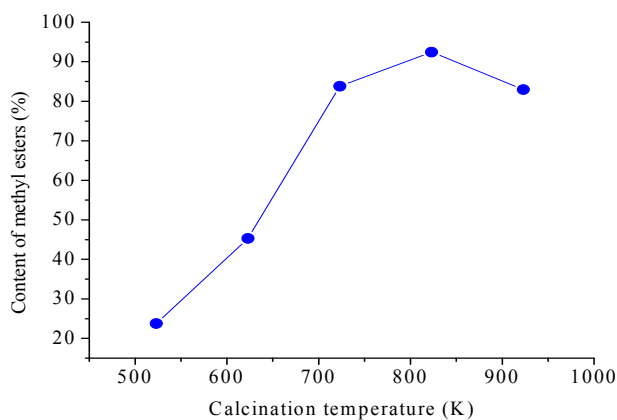### 3.3.2. Influence of Calcination Temperature
Figure 2 shows the influence of calcination temperature on the catalytic activity in the temperature range from 523 to 923 K. The optimal calcination temperature observed was 823 K. At this temperature, the methyl ester content reached 91.58%. However, when the calcination temperature increased to 923 K, the catalyst activity decreased. Such results are in line with the basicity properties shown in **Table 2**, indicating that higher basicity results in higher conversion and higher methyl ester content. However, the FAME content obtained using 47 wt.% CH_3COOK/artificial zeolite calcined at 523 K is lower than that obtained using 23 wt.% CH_3COOK/artificial zeolite calcined at 823 K, although the basicity of the former is higher than that of the latter (0.2540 vs. 0.1393 mmol KOH/g). This implies that basicity is the most important, but not the only factor affecting the activity of these supported catalysts.

3.4. FTIR Analysis

IR spectroscopy was used to investigate the CH_3COOK/artificial zeolite catalysts. The results are shown in **Fig. 3**. For the parent artificial zeolite, two absorption bands at

Table 3. Results of orthogonal experiment L9_3_4 for base-catalyzed transesterification and range analysis.

Experimental no.	Factors and levels			Experimental results
	A	B	C	Methyl ester content(%)
1	1	1	1	42.35
2	1	2	2	65.02
3	1	3	3	62.38
4	2	1	3	74.39
5	2	2	1	91.08
6	2	3	2	81.85
7	3	1	2	62.56
8	3	2	3	88.89
9	3	3	1	87.12
I	56.58	59.77	71.03	
II	82.44	81.66	75.51	
III	79.52	77.12	72.00	
R	25.86	21.90	4.48	

Figure 1. Influence of CH_3COOK loading on the content of methyl esters. Reaction conditions: methanol/oil molar ratio, 10:1; catalyst amount, 2wt.%; reaction time, 4h; and methanol reflux temperature.

Figure 2. Influence of calcination temperature on the content of methyl esters. Reaction conditions: methanol/oil molar ratio, 10:1; catalyst amount, 2wt.%; reaction time, 4h; and methanol reflux temperature.

3440 and $1650 cm^{-1}$ were attributed to stretching and bending vibrations of physically absorbed water, respectively. CH_3COOK/artificial zeolites catalysts calcined at high temperature (curves b, c, d, f and g in **Fig. 3**) showed intense absorption at approximately $3440 cm^{-1}$, which could be assigned to ν_{OH} stretching vibrations of hydroxyl groups attached to the support. Such hydroxyl groups are mainly formed by the reaction of surface-absorbed water with the support during the activation by calcination. [22] When the catalyst samples were calcined at higher temperatures (curves d, f and g in **Fig. 3**), there was very little absorbed water on the support surface. However, there was still a strong absorption peak at~$1650 cm^{-1}$. This indicates that the peak at $1650 cm^{-1}$ was mainly due to surface hydroxyl groups and that these surface OH groups were possibly active sites, as reported by Xie and Huang. [23]

Furthermore, the absorption broad band at ~$3440 cm^{-1}$ could be partly assigned to stretching vibrations of Al-O-K or Si-O-K groups. [24,25,26] According to Stork and Pott, [27] K^+ ions may replace the protons of hydroxyl groups attached to the support during activation. Thus, K^+ ions from CH_3COOK could form Al-O-K or Si-O-K groups by replacing the protons of hydroxyl groups attached to the artificial zeolites during activation by calcination, and can probably be considered to be another active basic species of this catalyst in transesterification.

As observed from **Fig. 3**, the absorption intensity at ~$3440 cm^{-1}$ increased with the CH_3COOK loading (curves b-d), indicating that an increase in basic sites resulted in an increase in catalytic activity, which is in accordance with the results shown in **Fig. 1**. On the other hand, the intensity of the abso0rption at $3440 cm^{-1}$ decreased at higher calcination temperatures (curves d, f and g), indicating a decrease in basic sites, in line with Hammett basicity measurement (**Table 2**). The absorption peak at ~$1552 cm^{-1}$ can be assigned to asymmetric vibration of COO^- [28] of CH_3COOK (curve e), which disappeared after calcination at 823K (curve d), demonstrating that CH_3COOK decomposed completely after calcination at 823 K. In addition, there were some other absorption peaks at ~$400-1400 cm^{-1}$ for all samples, which can be attributed to Al-O (or Si-O) symmetric stretching and ring vibration in Al-O and Si-O tetraheda formed through the oxygen atom.

3.5. XRD Analysis

XRD patterns of artificial zeolites and CH_3COOK/artificial zeolite samples with different CH_3COOK loading are shown in **Fig. 4**. The XRD pattern of artificial zeolites is irregular, which may be related to their structure. After calcination of artificial zeolites loaded with CH_3COOK, more regular and distinct diffraction peaks (* and □ in **Fig. 4**) appeared in the XRD patterns.
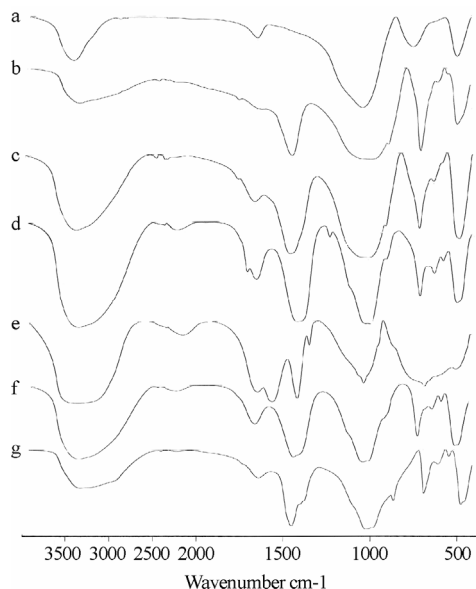
Figure 3. FTIR spectra: (a) artificial zeolites; (b) 33% CH_3COOK/artificial zeolites calcined at 823 K for 5 h; (c) 41% CH_3COOK/artificial zeolites calcined at 823 K for 5 h; (d) 47% CH_3COOK/artificial zeolites calcined at 823 K for 5 h; (e) 47% CH_3COOK/artificial zeolites without calcination; (f) 47% CH_3COOK/artificial zeolites calcined at 923 K for 5 h; and (g) 47% CH_3COOK/artificial zeolites calcined at 973 K for 5 h.
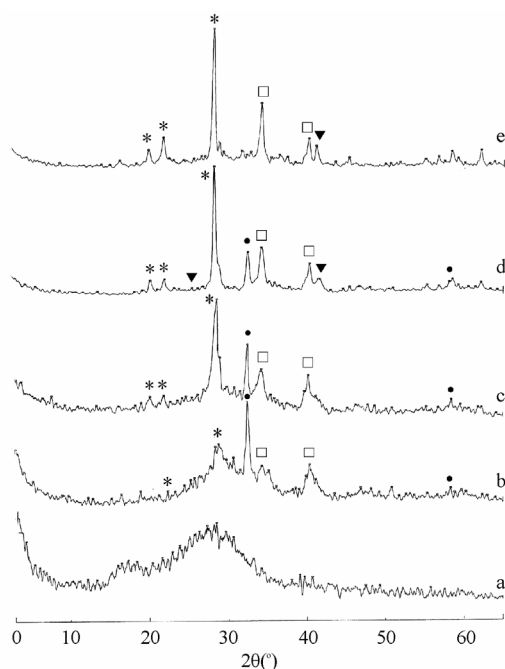

Figure 4. XRD patterns: (a) parent artificial zeolites; (b) 33% CH_3COOK/artificial zeolites calcined at 823 K for 5 h; (c) 41% CH_3COOK/artificial zeolites calcined at 823 K for 5 h; (d) 47% CH_3COOK/artificial zeolites calcined at 823 K for 5 h; and (e) 47% CH_3COOK/artificial zeolites calcined at 923 K for 5 h. * $KAlSiO_4$, Kalsilite; □ $K_{0.85}Na_{0.15}AlSiO_4$; ● $K_2Al_2O_4$; and ▼ K_2O.

This is possibly due to the reaction of CH_3COOK with the support during activation, resulting in the more regular and stable structure necessary for catalysis.

As shown in **Fig. 4**, when the CH_3COOK loading was below 47wt.% (curves b and c), the XRD patterns contained only diffraction peaks (2θ =20.5°,22.3°,28.6°, 34.6°,40.6°) assigned to new species formed by reaction between CH_3COOK and the support during the activation process. These diffraction peaks can probably be ascribed to two new species, KAlSiO4 (Kalsilite; *) and $K_{0.85}Na_{0.15}AlSiO_4$ (□), formed by the movement of K^+ from CH_3COOK into the crystal lattices of the support and subsequent reaction. There were no characteristic peaks for CH_3COOK or K_2O, probably due to good dispersion of K^+ derived from CH_3COOK on artificial zeolites in the form of various compounds, while a K_2O phase undetectable by XRD may have dispersed onto the artificial zeolite surface as a monolayer. [29] In addition, 2θ diffraction peaks at 32.8° and 58.6° can probably be ascribed to $K_2Al_2O_4$ (●), also obtained by reaction between K^+ and the support.

However, when the CH_3COOK loading increased to 47 wt.%, the characteristic XRD peaks of K_2O (2θ= 25.8°,41.9°) were detected (curve d in **Fig. 4**). According to the results shown in **Fig. 1** and **Table 2**, this K_2O species may account for the high catalytic activity and basicity of the catalyst, because 47% CH_3COOK/artificial zeolites calcined at 823K for 5h exhibited the highest catalytic activity and basicity. Furthermore, when the calcination temperature increased to 923K, the characteristic XRD peak at 2θ =32.8° vanished, presumably because $K_2Al_2O_4$ (●) was destroyed at higher calcination temperatures.

Taken together, the characterization results indicate that K_2O (derived from CH_3COOK) and surface hydroxyl groups, as well as Al-O-K (or Si-O-K) groups, were probably the active sites mainly responsible for the transesterification of *J. curcas* oil with methanol.

3.6. Optimization of the Transesterification Reaction

For the transesterification reaction, orthogonal experiments were carried out to determine the optimum reaction conditions. The effects of various factors on the reaction were also studied. The orthogonal scheme chosen and the data obtained are shown in **Table 3**.

As shown in **Table 3**, the extent to which the transesterification of *J. curcas* oil was affected in terms of the range (R) value was A＞B＞C, namely, oil/methanol ratio (A) first, followed by catalyst amount (B) and reaction time (C). Taking the FAME content into account, the optimum reaction conditions were $A_2B_2C_2$; namely, oil/methanol ratio, 1:10; catalyst amount, 2wt.%; and reaction time, 4h.

The molar ratio of *J. curcas* oil to methanol is the

most important factor affecting the transesterification to methyl esters (**Table 3**). Theoretically, three moles of methanol are required for one mole of triglyceride to yield one mole of glycerol and three moles of FAME. However, a slight excess of methanol is required to drive the equilibrium to the product side, because the transesterification reaction is reversible. [1] With an increase in the oil/methanol molar ratio, the conversion increased considerably. However, further addition of methanol not only had no significant effect on the conversion, but also seriously affected glycerine separation due to the increase in solubility. [30] Thus, the optimum molar ratio of *J. curcas* oil to methanol to produce methyl esters was 1:10.

The amount of catalyst is another important factor that affects the reaction. With no catalyst, transesterification does not occur. When the amount of catalyst was insufficient, the FAME content was very low (entries 1, 4, 7). Saponification took place when the amount of catalyst was increased to 3%, leading to product emulsion and making separation difficult. The FAME content and product yield were also influenced (entries 3, 6, 9). As revealed in orthogonal experiments, 2 wt.% catalyst was appropriate for this transesterification reaction.

The final factor affecting transesterification is the reaction time. When the reaction time is too short, the conversion of vegetable oil to methyl esters is incomplete, and conversion increases with the reaction time. However, when the reaction reaches equilibrium, prolonged reaction time does not increase the FAME content of the product, but increases the cost for biodiesel production. In homogeneous base-catalyzed transesterification, the reaction time is usually less than 1 h. For heterogeneous transesterification the reaction time needs to be longer, because the system components, the base catalyst, methanol and *J. curcas* oil in the present study, require a longer contact time. According to orthogonal experiments, an optimum reaction time of 4 h was chosen.

An experiment was carried out under above optimum reaction conditions, a product yield of 94.27% and methyl ester content of 91.58% were obtained after transesterification.

4. CONCLUSIONS

Easily prepared solid-base catalysts using artificial zeolites as a support were developed for the transesterification of *J. curcas* oil with methanol to produce biodiesel. The CH₃COOK/artificial zeolites solid catalysts exhibited high catalytic activity in the transesterification process. The methyl ester content exceeded 91% when the catalyst with 47 wt.% CH₃COOK was calcined at 823 K for 5 h. Catalyst characterization revealed that K_2O, surface hydroxyl groups and Al-O-K (or Si-O-K) groups are the main basic sites. Furthermore, the activity of the catalysts depends strongly on their basicity. Or-

thogonal experiments revealed the following optimum reaction conditions: oil/methanol ratio, 1:10; catalyst amount, 2wt.%; and reaction time, 4h. No water washing step is needed thus no waster water was produced during this process. The information mentioned above establishes certain basis for industrial biodiesel production from *J. curcas* seed oil using the heterogeneous catalysts. Further investigations on the reaction mechanism and active sites are under way in our laboratory.

REFERENCES

[1] Ma, F. and Hanna, M. A. (1999) Biodiesel production: A review. Bioresour Technol, **70**, 1−15.

[2] Ramadhas, A. S., Jayaraj, S. and Muraleedharan C. (2005) Biodiesel production from high FFA rubber seed oil. Fuel, **84**, 335−340.

[3] Schuchardt, U., Sercheli, R. and Vargas, R. M. (1998) Transesterification of vegetable oils: A review. J Braz Chem Soc, **9**, 199−210.

[4] Graboski, M. S. and McCormick, R. L. (1998) Combustion of fat and vegetable oil derived fuels in diesel engines. Prog Energy Combust Sci, **24**, 125−164.

[5] Watkins, R. S., Lee, A. F. and Wilson, K. (2004) Li-CaO catalysed tri-glyceride transesterification for biodiesel applications. Green Chem, **6**, 335−340.

[6] Xie, W. L. and Li, H. T. (2006) Alumina-supported potassium iodide as a heterogeneous catalyst for biodiesel production from soybean oil. J Mol Catal A: Chem, **255**, 1−9.

[7] Gryglewicz, S. (1999) Rapeseed oil methyl esters preparation using heterogeneous catalysts. Bioresour Technol, **70**, 249−253.

[8] Ono, Y. and Baba, T. (1997) Selective reactions over solid base catalysts. Catal Today, **38**, 321−337.

[9] Clark, J. H. and Macquarrie, D. J. (1996) Environmentally friendly catalytic methods. Chem Soc Rev, **25**, 303−310.

[10] Kim H J, Kang B S, Kim M J, Park Y M, Kim D K, Lee J S, Lee K Y. Transesterification of vegetable oil to biodiesel using heterogeneous base catalyst. Catal Today 2004; 93−95: 315−320.

[11] Xie, W. L., Peng, H. and Chen, L. G. (2006) Transesterification of soybean oil catalyzed by potassium loaded on alumina as a solid-base catalyst. Appl Catal A: Gen, **300**, 67−74.

[12] Bordawekar, S. V. and Davis, R. J. (2000) Probing the basic character of alkali-modified zeolites by CO_2 adsorption microcalorimetry, butene isomerization, and toluene alkylation with ethylene. J Catal, **189**, 79−90.

[13] Suppes, G. J., Dasari, M. A., Doskocil, E. J., Mankidy, P. J. and Goff, M. J. (2004) Transesterification of soybean

oil with zeolite and metal catalysts. Appl Catal A: Gen, **257**, 213−223.

[14] Doskocil, E. J. and Mankidy, P. J. (2003) Effects on solid basicity for sodium metal and metal oxide occluded NaX zeolites. Appl Catal A: Gen, **252,** 119−132.

[15] Leclercq, E., Finiels, A. and Moreau C. (2001) Trans-esterification of rapeseed oil in the presence of basic zeolites and related solid catalysts. J Am Oil Chem Soc, **78**, 1161−1165.

[16] Gubitz, G. M., Mittelbach, M. and Trabi, M. (1999) Exploitation of the tropical oil seed plant Jatropha curcas L. Bioresour Technol, **67**, 73−82.

[17] Forni, L. (1974) Comparison of the methods for the determination of surface acidity of solid catalysts. Catal Rev, **8**, 65−115.

[18] Gorzawski, H. and Hoelderich, W. F. (1999) Preparation of superbases and their use as catalysts for double-bond isomerization. J Mol Catal A: Chem, **144**, 181−187.

[19] Xie, W. L., Huang, X. M. and Li, H. T. (2007) Soybean oil methyl esters preparation using NaX zeolites loaded with KOH as a heterogeneous catalyst. Bioresour Technol, **98**, 936−939.

[20] Chen, Y. and Zhang, L. F. (1992) Surface interaction model of γ-alumina-supported metal oxides. Catal Lett, **12**, 51−62.

[21] Tanabe, K. (1985) Catalysis by acids and bases. in: B. Imelik, C. Nacceche, G. Condurier, Y. BenTaarti, J. C. Vedrine (Eds.), Elsevier, Amsterdam, 1−1.

[22] Nakamoto, K. (1970) Infrared spectra of inorganic and coordination compounds. John Wiley, New York, 98−98.

[23] Xie, W. L. and Huang, X. M. (2006) Synthesis of biodiesel from soybean oil using heterogeneous KF/ZnO catalyst. Catal Lett, **107**, 53−59.

[24] Krupay, B. W. and Amenomiya, Y. (1981) Alkali-promoted alumina catalysts: I. Chemisorption and oxygen exchange of carbon monoxide and carbon dioxide on potassium-promoted alumina catalysts. J Catal, **67**, 362−370.

[25] Iordan, A., Kappenstein, C., Colnay, E. and Zaki, M. I. (1998) Surface contribution to the interfacial chemistry of potassium modified oxide catalysts. J Chem Soc Faraday Trans, **94**, 1149−1156.

[26] Amenomiya, Y. and Pleizier, G. (1982) Alkali-promoted alumina catalysts: II. Water-gas shift reaction. J Catal, **76**, 345−353.

[27] Stork, W. H. J. and Pott, G. T. (1974) Studies of compound formation on alkali/γ-aluminum oxide catalyst systems using chromium, iron, and manganese luminescence. J Phys Chem B, **78**, 2496−2506.

[28] Bilger, S., Syskakis, E., Naoumidis, A. and Nickel, H. (1992) Sol-gel synthesis of strontium-doped lanthanum manganite. J Am Ceram Soc, **75**, 964−970.

[29] Jiang, D. E., Zhao, B. Y., Xie, Y. C., Pan, G. C., Ran, G. P. and Min, E. Z. (2001) Structure and basicity of γ-Al2O3-supported MgO and its application to mercaptan oxidation. Appl Catal A: Gen, **219**, 69−78.

[30] Meher, L. C., Sagar, D. V. and Naik, S. N. (2006) Technical aspects of biodiesel production by transesterification-a review. Renew Sust Energy Rev, **10**, 248−268.